Exergy and exergoeconomic assessment and multi-objective optimization of a renewable assisted CCHP system

MOHAMMAD HOSSEIN JAHANGIR[1,*], **ARMAN ZENDEHNAM**[2], **AND HAMED ALIMORADIYAN**[2]

[1] *Associate Professor, Faculty of New Sciences and Technologies, University of Tehran, Tehran, Iran*
[2] *Department of Renewable Energies and Environment Faculty of New Sciences & Technologies University of Tehran, Tehran, Iran*
[*] *Corresponding author: mh.jahangir@ut.ac.ir*

Manuscript received 13 January, 2021; revised 19 September, 2021; accepted 27 September, 2021. Paper no. JEMT-2101-1274.

The current study analyzed and optimized a renewable-assisted multi-generation system in energy, exergy, and exergoeconomic. The proposed system is composed of PTCs, a horizontal-axis wind turbine, an organic Rankine cycle, heat recovery heat exchangers, a parallel double-effect LiBr-H_2O absorptive chiller, heat recovery heat exchangers, and an electrolyzer. The designed system has been being used for the simultaneous production of electricity, heating, cooling, and hydrogen. Moreover, a thermodynamic model of the defined system has been developed in engineering Equation Solver (EES) software. A Genetic Algorithm (GA) model was also conducted to find the optimum composition of decision variables that efficiently optimize the system performance in terms of cost and exergy. A sensitivity analysis also has been applied to measure the effect of decision variables on the exergoeconomic performance of the proposed system. Results show that rising the inlet flow rate and inlet flow temperature to the Organic Rankin Cycle (ORC) turbine has an upward effect on the system's exergy efficiency and production cost rate. In addition, it was found that the increase of the boiler pressure only increases the exergy efficiency to a certain degree, and the exergy efficiency of the proposed system reduces in the pressures above 2600 kPa. With the optimization of the decision variables using a GA model, it was found that there is room to enhance the exergy exploitation rate by 2.6% and reduce the total rate of the production cost of the proposed system by 12.9%.

keywords: *Energy, exergy, exergoeconomic, multi-generation system, multi-objective optimization, sensitivity analysis, exergy efficiency*

http://dx.doi.org/10.22109/jemt.2021.267289.1274

1. INTRODUCTION

Nowadays, the worldwide trend to eliminate fossil energy resources and replace renewable energies in energy production systems has been remarkably raised [1]. The cogeneration systems are crucial energy systems for the enhancement of energy efficiency, energy security, and reduction of energy losses in the distribution systems all around the world. These systems are the best choices for the high-energy demanding areas which need various types of energy carriers. Since these systems have been historically designed to consume fossil fuels for power generation, incorporating renewables in such systems and supplying their primary energy demand from environmentally friendly solar and wind energies can profoundly reduce their harmful environmental effects and further sustainability [2–5]. Ahmadi et al.[6] have conducted a thermodynamic analysis over a system for the combined production of electricity, heating, and cooling. The proposed system is composed of a gas turbine, an organic Rankine cycle, a single-effect absorption chiller, and a water heater system. Based on the exergy analysis, it is evident that the exergy efficiency of the tri-generation system is considerably higher than the cogeneration (heat and power) system. Findings also suggest that the cogeneration system is more efficient than the single gas-turbine cycle, at least from the energetic point of view. Buck and Friedmann [7] have exergetically studied a tri-generation system encompassing a small solar system and a micro-wind turbine. Comparing the performance of a single effect absorption refrigeration cycle (SEARC) with a double effect absorption refrigeration cycle (DEARC) revealed that the DEARC is a more economically viable alternative as it provides higher energy efficiency and substantially higher energy efficiency by decreasing the operational costs of the proposed system. Al-Sulaiman et al. [8] have analyzed the exergetic perfor-

mance of a tri-generation system composed of linear parabolic trough collectors (PTCs), an organic Rankine cycle, a SEARC, and heat-exchanger as a means for energy production. The analysis shows that the system can achieve an exergy efficiency of up to 20% using the PTCs without any storage system. However, incorporating the storage devices in the proposed system may cause lower exergy efficiency by 12-13% and weaken the system performance from an exergetical viewpoint. Results reveal that the PTCs and the Rankine cycle evaporators are significant sources of exergy losses in the proposed system. Gomri [9] compared the performance of a single effect absorption cooling system and a double effect absorption cooling cycle in terms of exergy. Considering the same inlet/outlet temperatures for both systems, the latter has provided superior exergy in this study. Iranmanesh and Mehrabian [10] have thermodynamically evaluated a double-effect LiBr-H2O absorption refrigeration cycle and checked the impact of modeling parameters on the exergy performance of the system. Analysis suggests that the efficiency rate of high-temperature heat exchangers is of more importance than the low-temperature heat exchangers when it comes to exergitical efficiency. Salehzadeh et al. [11] have conducted an exergy analysis over a tri-generation system and analyzed the effects of various parameters on the exergy performance of the proposed system. Findings suggested that the compressor pressure and pre-heater temperature optimization are the main driving factors of the exergy efficiency in the designed system. An overview of the existing micro-trigeneration systems has been conducted by Sonar et al. [12]. They pointed out the waste heat utilization in these systems for heating and cooling products as the most attractive features of the micro-trigeneration systems. The incorporation of heat recovery technologies in such systems provides energy efficiency of up to 80% and considerably reduces their environmental impacts to a large extent. Therefore, the micro-trigeneration system is a viable alternative for residential building applications. Anvari et al. [13] have exergitically evaluated a gas turbine-based tri-generation cycle to identify the exergy losses in the modeled system. Based on the outcomes, about 29% of exergy losses in this system and most of the exergy losses in the proposed system are due to the pre-heater rather than the other components. Noorpoor and Heidararabi [14] have conducted an exergy analysis to evaluate the performance of a tri-generation system for building applications. The proposed system is composed of an organic Rankine cycle, an absorptive chiller, and a heat recovery cycle. Results suggest that the heat exchanger in the Rankine cycle, the cooling tower, absorption column, and the evaporators are the weakest areas in terms of exergy efficiency in the mentioned system. Mousafarash [15] has implemented an exergo-environmental analysis over a tri-generation system encompassing a gas-turbine and double-effect steam absorption chillers and evaluated the impact of some parameters such as the compressor pressure, inlet and outlet gas-turbine temperature, isentropic efficiency of the gas-turbine, and temperature of the absorptive chillers. Analysis insists on the superiority of the tri-generation and cogeneration systems compared to the single gas-fired turbine from both an exergitical and environmental point of view. Eisavi et al. [16] proposed and analyzed a novel solar-assisted tri-generation system. The modeled system encompasses an organic Rankine cycle, a double-effect water-lithium bromide absorption refrigeration cycle, and heat exchangers to simultaneously produce electricity, heating, and cooling. Results show that substitution of the double effect absorption cooling system from the single effect absorption cooling system raises the cooling production capacity of the proposed system to 48.5% and the system's total efficiency to 96%. The inlet and outlet temperatures to/from the water pump in the Rankine cycle have reportedly been identified as the primary determinant of the exergy in the designed system. Ahmadi et al. [17] have exergitically studied a biomass-based multi-generation energy system that simultaneously produces electricity, heating, cooling, hot water, and hydrogen. The proposed system is liked an organic Rankine cycle, an electrolyzer, and a single effect chiller. Results show that the highest irreversibility rate exists in the combustion chamber and the evaporator of the Rankine cycle. Moreover, an environmental analysis conducted in this study reveals that the environmental impacts of the multi-generation system are substantially lower than the combined heat and power production system. In another study, they adopted an exergy analysis over a novel, sophisticated multi-generation system, composed of a micro gas-turbine, heat recovery steam generator with double pressure levels, single effect absorber chiller, water heater, and ion-partitioning membranes and simultaneously produce electricity, heating, cooling, hot water, and hydrogen. A multi-objective optimization algorithm has been conducted in this study to reach the best composition of design parameters that provide the highest exergy efficiency for the designed system. Al-Ali and Dincer [18] have conducted a thermodynamical analysis over a multi-generation system that uses solar and geothermal energy as its primary energy source. The system can simultaneously produce electricity, heating, cooling, and hot water for industrial purposes. While the energy and exergy efficiencies of the conventional single generation system were 16.4 and 26.2%, respectively, the figures for the multi-generation system obtained 78 and 36.6%. Malik et al. [19] have exergitically evaluated a renewable-based multi-generation system that is highly suitable for residential applications. The proposed system uses several resources such as biomass and geothermal energy sources. It produces five various products to meet the energy demand of a residential building. The system is composed of a single effect absorber chiller, an organic Rankine cycle, and some multi-stage steam turbines. Evaluations indicate that the system at the best performance provides the energy and exergy efficiency of 56.5 and 23%, respectively; also, the analysis identifies the combustion chamber as the most exergy-destructive component in the proposed system. Ozlu and Dincer [20] have proposed and assessed a novel multi-generation system that works based on solar and wind energy. Several exergy analyses reveal that the system can simultaneously produce 48 KW electricity, 28 KW cooling, 298.5 KW heating, and about 1.96 kg/hr hydrogen. Findings suggest the proposed multi-generation system's superiority over the tri-generation system in terms of both energy and exergy aspects. Yılmaz et al. [21] have evaluated the performance of a high-pressure condenser in a double-effect lithium bromide-water absorption system. Results show that optimizing the temperature of the high-pressure condenser has the highest improving effect on the exergitical performance of the system. The mentioned modeling factors are of such importance that raising the condenser temperature by 2 C may improve the exergy efficiency of the system by 9.72-35.09%. Maryami and Dehghan [22] have conducted an exergy analysis over some LiBr/water absorption refrigeration systems. They have evaluated the impact of diverse parameters on the exergitical performance of half effect, single-effect, double effect, parallel double effect, and triple effect absorption refrigeration system. It was revealed that rising the generator temperature has the most destructive effect on the exergitical performance of all studied systems. Moghimi et al. [23] have exergitically analyzed and

optimized the performance of a gas-turbine-based tri-generation system using a multi-objective optimization algorithm. Several parameters such as turbine inlet temperature, the pressure ratio of the compressor, pinch point temperature, and the coefficient of performance (COP) of the chiller have been selected for optimization in this study. Analysis shows a 7% improvement in the exergy efficiency of the system with the optimization of the identified factors. The same study has been conducted by Yang et al. [24] on a solar hybrid combined cooling heating and power (CCHP) to optimize the system's performance. They have considered the compressor pressure ratio, turbine inlet temperature, and pressure, efficiency rate of the heat exchangers as inputs for the optimization algorithm. With optimizing the system performance, the exergy efficiency in the maximum heating production state obtained 53.1%; the figure for the maximum cooling production state for the system was about 45.36%. Another study has been conducted by Sezer and Muammer [25] over a multi-generation system that uses wind energy in a combination of solar energy as the energy source. Instead of PTCs, they used concentrated photovoltaic thermal (CPVT) collectors in the proposed system. Like the previous study, the results indicate that rising the ambient temperature has a destructive impact on the exergitical performance of the proposed system. Additionally, the CPVTs also have been identified as the primary source of exergy destruction in this system. Yilmaz et al. [26] have developed and evaluated a novel solar-assisted multi-generation system energetically and exergitically. The proposed system includes parabolic dish concentrators with heat storage, an organic Rankine cycle, a double-effect LiBr/water absorptive chiller, heat exchangers, and an electrolyzer. The system suggests about the same energy and exergy efficiencies in most cases (about 45%). Contrary to the previous studies, raising the ambient temperature brings about an improving effect on the exergitical performance of the proposed system.

A. State of Purpose

Due to the great importance of clean solar energy for power generation, heating/cooling purposes, and hydrogen production, this paper aims to propose and analyze a Multi-generation system integrated into a horizontal-axis wind turbine and a Rankine vapor cycle that uses solar and wind energy sources for synchronous production of electricity, heating, cooling, and hydrogen. To create a crystal clear view of the system, the excess steam from the Rankine vapor cycle is utilized in an absorptive chiller and a heat recovery system to produce the heating and cooling load in the proposed system. An electrolyzer also has been incorporated into the system as a means for hydrogen production to enhance the applicability of the suggested system. The electrolyzer in the system acts as an energy storage device to supply energy during the unavailability periods of solar energy. The large-scale vapor Rankine cycles are generally sophisticated systems that have historically been the center of attention for worldwide power generation. Since these systems are energy-efficient and widely used for power generation in the last decades, the large-scale vapor Rankine cycles are virtually capital-intensive. They need a wealth of fortune for their installation. These systems cannot be considered the best alternatives for low-capacity purposes, and their application is mainly restricted to large-scale facilities. Organic Rankine cycles offer a viable option compared to the traditional vapor Rankine cycles, at least for low capacity purposes. This paper adopts an up-to-date exergy-economic analysis to identify the critical points in the proposed multi-generation system from an exergetic and economic point of view. The proposed system is a multi-generation system for simultaneous production of electricity, heating, cooling, and hydrogen, which is linked to parabolic trough collectors (PTCs), a horizontal-axis wind turbine, an organic Rankine cycle, heat recovery heat exchangers, a parallel double-effect LiBr-H2O absorptive chiller, heat recovery heat exchangers, and an electrolyzer in a different form with the old researches. Furthermore, an optimization is performed based on a code developed in the EES software program. Multi-objective optimization is finally performed using a genetic evolution algorithm to enhance the exergy efficiency and reduce the energy production cost in the proposed system.

2. SYSTEM DESCRIPTION

Figure 1 illustrates the schematic diagram of the multi-generation system studied in this paper. The proposed system simultaneously produces electricity, heating, cooling, and hydrogen using solar and wind energy as its primary energy source. It comprises parabolic trough collectors (PTCs), a horizontal-axis wind turbine, an organic Rankine cycle, a heat exchanger, a double effect LiBr/water absorptive chiller, and an electrolyzer for hydrogen production.
The PTCs in the proposed system uses Therminol-66 as their working fluid, which is insignificantly sensitive to temperature fluctuations.

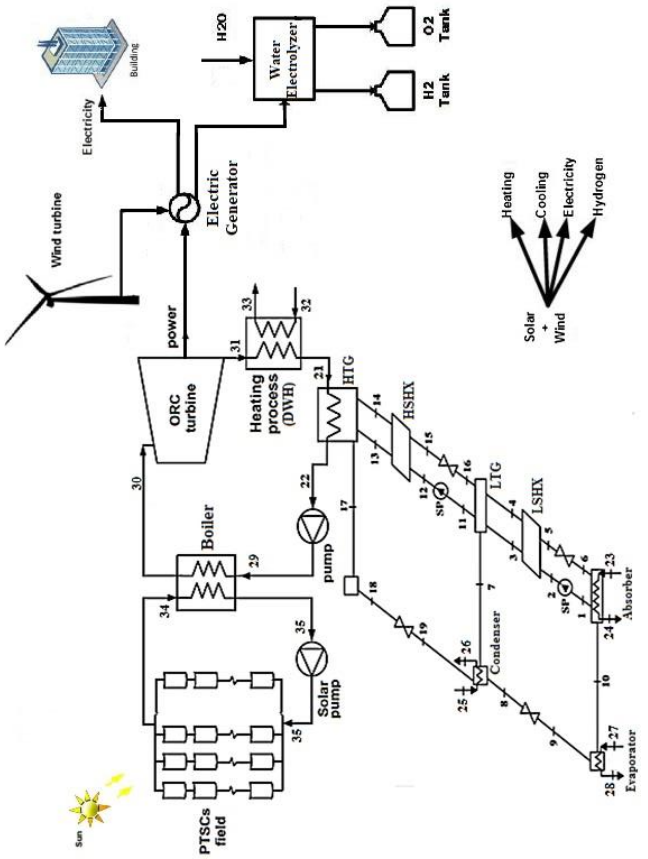

Fig. 1. schematic of the Proposed Multi-generation System

Expansion of the super-heated working fluid in the Rankine cycle turbine produces a considerable proportion of electricity

in this system. A significant proportion of the electricity also is produced by the horizontal-axis wind turbine. A portion of the produced electricity is then used in the electrolyzer for hydrogen production. After the expansion in the turbine, the n-Octane is then transferred to a heat exchanger that provides hot water in the system. The working fluid afterward enters the high-temperature generator of the absorptive chiller and provides the requiring driving force for the cooling production. Saturated n-Octane is then pressurized and pumped to the boiler. The absorptive chiller uses Li-Br as the working fluid based on three diverse levels of pressure, low pressure, medium pressure, and high-pressure conditions. The high-temperature generator works under high pressure, the condenser and low-temperature generator work under medium pressure, and the evaporator and absorbent work under low-pressure conditions. Exiting saturated working fluid from the evaporator is absorbed by the Li-Br in the absorption column. The absorption of steam during this process attenuates Li-Br and weakens the absorption performance of the working fluid. Therefore, the working fluid is then pumped to the high-temperature generator for regeneration. A significant proportion of vapor is desorbed in the high-temperature generator. The working fluid then enters the high-temperature heat exchanger to transfer heat with dilute working fluid. Passing from an expansion valve, the working fluid loses temperature and pressure and then is transferred to the low-temperature generator. The excess vapor is desorbed during this process, and the working fluid is regenerated to reach a certain degree of intensity. Passing from the low-temperature heat exchanger and the expansion valve, the working fluid finally returns to the absorption column. Exiting vapor from the low-pressure generator is condensed in the condenser and passes from an expansion valve to enter the evaporator. Heat transfer between exiting vapor and the inlet water to the evaporator generates cooling capacity in the proposed system.

3. SYSTEM MODELING

Engineering Equation Solver (EES) software has been used in this study to scrutinize the exergitical performance of the proposed system. Several assumptions have been considered to simplify the sophisticated thermodynamic model as following [27],

- Modeling is performed under steady-state conditions.
- The variation of potential and kinetic energies is insignificant.
- Pressure and heat losses in the cycle components are insignificant.
- The variation of enthalpy in the expansion valves is insignificant.
- The energy consumption of the pumps in the refrigeration system is insignificant.
- Working fluids exiting from the condensers are fully saturated fluids.
- Working fluids exiting from the evaporators are fully saturated vapors.
- The turbine and the pumps are considered isentropic.
- The analysis is conducted under atmospheric pressure at 298.15 K.

Table 1 provides the thermodynamic properties of Therminol-66. Therminol-66 absorbs the sun heat using the PTCs and transfer the collected heat to the working fluid of the Rankine cycle, n-Octane.

Table 1. Thermodynamic properties of Therminol-66

Density (25^oC)	1005 kg$/m^3$
Viscosity (40^oC)	29.6(mm^2/s)
Boiling point	359^oC
Acceptable temperature interval	$0-354^oC$
Critical temperature	569^oC

Table 2 contains the thermodynamic properties of n-Octane. n-Octane absorbs the transferred heat in the boilers and becomes super-heated before entering the turbine.

Table 2. Thermodynamic properties of n-Octane

Chemical formula	C8H18
Melting point	-57^oC
Boiling point	$125-127^oC$
Density (25^oC)	70g$/ml$
Critical pressure	24.3 bar

A. Thermodynamic Analysis

In combination with the first and second laws of thermodynamics, the law of conservation of mass is adopted to analyze the performance of system components thermodynamically. Each element in the proposed system is considered a control volume, and the inlet and outlet mass/heat flow to/from them are entirely determined.

B. Energy Analysis

According to the law of conservation of mass, the mass is a non-degenerated feature of the substances which remain constant in every chemical reaction. Therefore, all of the inlet/outlet flow to/from and the producing mass inside the control volumes must be considered in the analysis. Considering a steady-state flow for the system components, the law of conservation of mass is defined as following [9],

$$\sum \dot{m}_i = \sum \dot{m}_o \quad \textbf{(1)}$$

$$\sum \dot{m}_i.x_i = \sum \dot{m}_o.x_o \quad \textbf{(2)}$$

Where $\dot{m}$ is the mass flow rate, and x is the Li-Br intensity. I in the above equations refers to the inlet flows, and o refers to the outlet flows to/from the control volume.
Based on the energy conservation law, the total energy of an isolated control volume remains constant. Therefore, any energy change in a control volume is due to the inlet and outlet energy flows into/from the control volume. Regardless of the potential and kinetic energy, the equation expressing conservation of energy in the control volumes is defined as follow,

$$\dot{Q} + \sum \dot{m}_i.h_i = \dot{W} + \sum \dot{m}_o.h_o \quad \textbf{(3)}$$

Where $\dot{W}$ and$\dot{Q}$ represent the required work and heat, i and o stand for the enthalpies of the inlet and outlet flows. With this definition, the energy efficiency rate of the proposed system for electricity production is defined as follows,

$$Q_{cooling} = A_{cooling}/25 \quad \textbf{(4)}$$

$\dot{W}_{net}$and$\dot{Q}_in$ in the above equation represents the net produced work in the Ranke cycle and the total input heat rate to the multi-generation system. $\dot{W}in$ is defined as the difference between the produced work in the turbine and the utilized energy in the pump:

$$\dot{W}_{net} = \dot{W}_{turbine} - \dot{W}_{pump} \quad \textbf{(5)}$$

$$\eta_{cog,h} = \frac{\dot{W}_{turbine} + \dot{Q}_{heat}}{\dot{Q}_{in}} \quad \textbf{(6)}$$

Where $\dot{Q}_{heat}$ represents the production heat for hot water production.)$\eta_{cog,h}$ also stands for the cogeneration efficiency for the simultaneous production of hot water and electricity [15]. The efficiency of the system for the cogeneration of cooling and power, $\eta_{cog,h}$, is defined as,

$$\eta_{cog,c} = \frac{\dot{W}_{net} + \dot{Q}_{evap}}{\dot{Q}_{in}} \quad \textbf{(7)}$$

Where $\dot{Q}_{heat}$is the production rate of cooling in the proposed system [16]. The efficiency of the tri-generation system, η_{trig}, for production of electricity, heating, and cooling is defined as follow,

$$\eta_{trig} = \frac{\dot{W}_{net} + \dot{Q}_{evap} + \dot{Q}_{heat}}{\dot{Q}_{in}} \quad \textbf{(8)}$$

Regarding the horizontal-axis wind turbine, the average power output can be calculated using the following equation[20]:

$$\dot{W}_{wind} = 1/2 \times \eta_{windturbine} \times \rho_{air} \times A_{windturbine} \times C_{pt} \times V^3 \quad \textbf{(9)}$$

Where $\eta_{windturbine}$represents the wind turbine efficiency, ρ_{air} is the air density, $A_{windturbine}$ is the wind turbine surface area, C_{ptis} the turbine power factor, and $V$is the average wind velocity. For the horizontal-axis wind turbines, the active surface area can be calculated using the following equation:

$$A_{windturbine} = \pi \times \frac{D^2}{4} \quad \textbf{(10)}$$

Where D is the nominal diameter of the wind turbine. The mass flow rate of the producing hydrogen in the electrolyzer is computed using the following equation,

$$\dot{m}_{H_2} = \frac{\eta_{Electrolyzer} \times (\dot{W}_{net} + \dot{W}_{wind})}{LHV_{H_2}} \quad \textbf{(11)}$$

Where $\eta_{Electrolyzer}$ is the electrolyzer's efficiency and LHV_{H2} represents the lower heating value of hydrogen. The efficiency of the system for multi-generation of electricity, heating, cooling, and hydrogen is defined as follow,

$$\eta_{multi} = \frac{\dot{W}_{net} + \dot{W}_{wind} + \dot{Q}_{evap} + \dot{Q}_{heat} + (\dot{m}_{H_2} \times LHV_{H_2})}{\dot{Q}_{in} + \dot{W}_{wind}} \quad \textbf{(12)}$$

COP of the absorptive refrigeration cycle also is calculated as follow,

$$COP = \frac{\dot{Q}_{evap}}{\dot{Q}_{gen} + \dot{W}_p} \quad \textbf{(13)}$$

Where $\dot{Q}_{evapand}$and$\dot{Q}_{gen}$ are the cooling capacity of the evaporator and the heat transfer rate to the generator. The efficiency of the low-temperature and high-temperature heat exchangers also are defined using the following equations:

$$\varepsilon_{LSHX} = \frac{T_4 - T_5}{T_4 - T_2} \quad \textbf{(14)}$$

$$\varepsilon_{HSHX} = \frac{T_{14} - T_{15}}{T_{14} - T_{12}} \quad \textbf{(15)}$$

C. Exergy Analysis

Just like the energy balance equation, the exergy equation is composed of diverse components. In the absence of nuclear, magnetic, and electric fields, and with consideration of no surface tension, the exergy equation for a given process is defined as follow,

(16)

Where Ex^K is the kinetic exergy, Ex^P is the potential exergy, and Ex^{CH} represents the chemical exergy which is calculated using the following equations:

$$\dot{E}x^{ph} = \dot{m}[(h - h_0) - T_0(s - s_0) \quad \textbf{(17)}$$

$$\dot{E}x^{ch} = \sum_{i=1}^{N} e^{ch}{}_{xi} + RT(\sum_{i=1}^{N} y_i \ln(y_i)) \quad \textbf{(18)}$$

s_0,h_0,T_0in the above equations represent entropy, enthalpy, and temperature in the environment. As the kinetic and potential energies for a given process are the same as kinetic and potential energies, Ex^K and Ex^P can be defined as follow,

$$Ex^k = 1/2 \times m \times v^2 \quad \textbf{(19)}$$

$$Ex^p = mgz \quad \textbf{(20)}$$

The following equation represents the exergy balance for a given process:

$$\dot{X}_q + \dot{X}_i = \dot{W} + \dot{X}_0 + \dot{X}_D \quad \textbf{(21)}$$

Where $\dot{X}_q$,$\dot{X}_D$, $\dot{W}$, represents exergy rate of work, exergy destruction rate, and exergy rate of heat transfer. Therefore, the exergy efficiency of the system can be defined as follows, The following equation represents the exergy balance for a given process:

$$\eta_{ex} = 1 - \frac{\dot{X}_D}{\dot{X}_F} \quad (22)$$

When it comes to only electricity production, the exergy efficiency is calculated using the following equation:

$$\eta_{ex,el} = \frac{\dot{W}_{net}}{\dot{X}_{in}} \quad (23)$$

Where $\dot{W}_{net}$ and $\dot{X}_{in}$ represents the rate of the net produced work and the inlet exergy to the system. For cogeneration of electricity and heating, $\eta X_{ex,cog,h}$ is defined as following [16],

$$\eta_{ex,cog,h} = \frac{\dot{W}_{net} + \dot{m}_{32}(\dot{X}_{33} - \dot{X}_{32})}{\dot{X}_{in}} \quad (24)$$

While for the cogeneration of electricity and cooling, $\eta X_{cog,c}$ is calculated using the following equation [15]:

$$\eta_{ex,cog,c} = \frac{\dot{W}_{net} + \dot{m}_{27}(\dot{X}_{27} - \dot{X}_{28})}{\dot{X}_{in}} \quad (25)$$

For trigeneration of electricity, heating, and cooling, $\eta X_{ex,trig}$ is defined as [8],

$$\eta_{ex,trig} = \frac{\dot{W}_{net} + \dot{m}_{32}(\dot{X}_{33} - \dot{X}_{32}) + \dot{m}_{27}(\dot{X}_{27} - \dot{X}_{28})}{\dot{X}_{in}} \quad (26)$$

Regarding the wind turbine and electrolyzer, the mean rate of exergy production is calculated using the following equation:

$$\dot{X}_{wind} = 1/2 \times \rho_{air} \times A_{windturbine} \times V^3 \quad (27)$$

$$\dot{X}_{H_2} = \dot{m}_{H_2} \times (\frac{235153}{MW_{H_2}} \times ex_{ch})_{H_2} \quad (28)$$

Considering the abovementioned equations, the total rate of exergy efficiency for the proposed multi-generation system is defined as,

$$\eta_{ex,multi} = \frac{\dot{W}_{net} + \dot{W}_{wind} + \dot{m}_{32}(\dot{X}_{33} - \dot{X}_{32}) + \dot{m}_{27}(\dot{X}_{27} - \dot{X}_{28})}{\dot{X}_{in} + \dot{X}_{wind}} \quad (29)$$

Table 3 and Table 4 provide the energy balance and exergy balance equations for each component of the multi-generation system.

Table 3. Energy balance equations for the system components

Component	Energy Balance Equation
Horizontal-axis wind turbine	$\dot{W}_{\text{wind}} = \frac{1}{2} * \eta_{\text{wind tuvbine}} * \rho_{\text{air}} * A_{\text{wind turbine}} * C_{pt} * V^3$
PTC	$\dot{Q}_{\text{in}} = \dot{m}_{34}(h_{34} - h_{35})$
ORC turbine	$\dot{m}_{30}h_{30} = \dot{m}_{31}h_{31} + \dot{W}_{\text{turbine}}$
Boiler	$\dot{m}_{34}(h_{34} - h_{34}) = \dot{m}_{29}(h_{30} - h_{29})$
ORC pump	$\dot{m}_{29}h_{29} = \dot{m}_{22}h_{22} + \dot{W}_{\text{pump}}$
Water heater exchanger	$\dot{m}_{31}(h_{31} - h_{21}) = \dot{m}_{32}(h_{33} - h_{32})$
Electrolyzer	$\eta_{\text{Electrolyzer}} * (\dot{W}_{\text{net}} + \dot{W}_{\text{wind}}) = \dot{m}_{H2}LHV_{H2}$
High-temperature generator	$\dot{Q}_{HTG} = \dot{m}_{17}h_{17} + \dot{m}_{14}h_{14} - \dot{m}_{13}h_{13}$
Low-temperature generator	$\dot{m}_3h_3 + \dot{m}_{16}h_{16} + \dot{m}_{17}h_{17} = \dot{m}_4h_4 + \dot{m}_{18}h_{18} + \dot{m}_7h_7 + \dot{m}_{11}h_{11}$
Condenser	$\dot{Q}_{\text{Cond}} = \dot{m}_7h_7 + \dot{m}_{19}h_{19} - \dot{m}_8h_8$
High-temperature heat exchanger	$\dot{m}_{14}h_{14} - \dot{m}_{15}h_{15} = \dot{m}_{12}h_{12} - \dot{m}_{13}h_{13}$
Low-temperature heat exchanger	$\dot{m}_4h_4 - \dot{m}_5h_5 = \dot{m}_2h_2 - \dot{m}_3h_3$
Absorber	$\dot{Q}_{\text{Abs}} = \dot{m}_{10}h_{10} + \dot{m}_6h_6 - \dot{m}_1h_1$
Evaporator	$\dot{Q}_{\text{Evap}} = \dot{m}_{10}h_{10} - \dot{m}_9h_9$

D. Exergoeconomic Analysis

This section provides an exergoeconomic analysis of the proposed system to better understand costs in the proposed system. Such analysis is of significant importance in decision-making for the selection of the system components. For the cost analysis, the cost balance equation is determined as follow,

$$\dot{Z}^{cl}_{total} + \dot{Z}^{om}_{total} + \dot{C}_{F,total} = \dot{C}_{p,total} \quad (30)$$

In this equation, the system product cost rate, $\dot{C}_{P,total'}$ is the sum of fuel cost rate, $\dot{C}_{F,total}$, initial investment cost rate, $\dot{Z}^{Cl}_{total}$, and maintenance cost rate, $\dot{Z}^{OM}_{total'}$.also is defined as the summation of the initial investment cost and maintenance cost rates. Considering the annual inflation rate, $\dot{Z}_k$for each component can be defined as following [28],

$$\dot{Z}_k = \frac{Z^{cl}_k \times \varphi \times \frac{i\times(1+i)^N}{(1+i)^N - 1}}{M \times 3600} \quad (31)$$

Table 4. Exergy balance equations for the system components.

Component	Energy Balance Equation
Horizontal-axis wind turbine	$\dot{X}_{D,\text{ wind turbine}} = \left(\frac{1}{C_{pt}} - 1\right) * \dot{W}_{\text{wind}}$
PTC	$\dot{X}_{\text{in}} = A_C I_C \left(1 + \frac{1}{3}\left(\frac{T_0}{T_s}\right)^4 - \frac{4}{3}\left(\frac{T_0}{T_s}\right)\right)$, $\dot{X}_{\text{D, collector}} = \dot{X}_{\text{in}} - \dot{m}_{34}\,(ex_{34} - ex_{35})$
ORC turbine	$\dot{X}_{D,\text{ turbine}} = \dot{m}_{30}\,\text{ex}_{30} - \dot{m}_{31}\,\text{ex}_{31} - \dot{W}_{\text{turbine}}$
Boiler	$\dot{X}_{D,\text{ Boiler}} = (\dot{m}_{34}(\,\text{ex}_{34} - \,\text{ex}_{34}) - \dot{m}_{29}\,(ex_{30} - ex_{29}))$
ORC pump	$\dot{X}_{D,\text{ pump}} = \dot{W}_{\text{pump}} + \dot{m}_{22}\,\text{ex}_{22} - \dot{m}_{29} ex_{29}$
Water heater exchanger	$dotX_{D,DWH} = \dot{m}_{31}\,(ex_{31} - ex_{21}) - \dot{m}_{32}\,(ex_{33} - ex_{32})$
Electrolyzer	$\dot{X}_{D,\text{ Electrolyzer}} = (\dot{W}_{\text{net}} + \dot{W}_{\text{wind}}) + (\dot{m}_{H2O} * ex_{H2O}) - \dot{X}_{H2}\text{a}$
High-temperature generator	$\dot{X}_{D,HTG} = \dot{m}_{13} ex_{13} - \dot{m}_{14} ex_{14} + \dot{m}_{21} ex_{21} - \dot{m}_{22} ex_{22} \dot{m}_{17}\,\text{ex}_{17}$
Low-temperature generator	$dotX_{D,LTG} = \dot{m}_{17}\,\text{ex}_{17} - \dot{m}_{18}\,\text{ex}_{18} + \dot{m}_{16} ex_{16} - \dot{m}_4 ex_4 + \dot{m}_3 ex_3 - \dot{m}_7 ex_7] - \dot{m}_{11} ex_{11}$
Condenser	$\dot{X}_{D,\text{ Cond}} = \dot{m}_7\,\text{ex}_7 + \dot{m}_{19}\,\text{ex}_{19} - \dot{m}_8\,\text{ex}_8 + \dot{m}_{25}\,\text{ex}_{25} - \dot{m}_{26}\,\text{ex}_{26}$
High-temperature heat exchanger	$\dot{X}_{D,HSHX} = \dot{m}_{14}\,\text{ex}_{14} - \dot{m}_{15}\,\text{ex}_{15} + \dot{m}_{12}\,\text{ex}_{12} - \dot{m}_{13}\,\text{ex}_{13}$
Low-temperature heat exchanger	$\dot{X}_{D,LSHX} = \dot{m}_4\,\text{ex}_4 - \dot{m}_5\,\text{ex}_5 + \dot{m}_2\,\text{ex}_2 - \dot{m}_3\,\text{ex}_3$
Absorber	$\dot{X}_{D,\text{ Abs}} = \dot{m}_{10}\,\text{ex}_{10} + \dot{m}_6\,\text{ex}_6 - \dot{m}_1\,\text{ex}_1 + \dot{m}_{23}\,\text{ex}_{23} - \dot{m}_{24}\,\text{ex}_{24}$
Evaporator	$\dot{X}_{D,\text{ Evap}} = \dot{m}_9 ex_9 - \dot{m}_{10} ex_{10} \dot{m}_{27} ex_{27} + \dot{m}_{28} ex_{28}$

φ in the above equation in the maintenance coefficient, which has been set to be 1.06 in this study. N represents the system life span, which is considered to be 20 years in this paper. I stands for the interest rate, and M is the total operating time of the system in a fiscal year. i and M have been assumed to be 10% and 7446 hr, respectively.

E. Optimization Algorithm

Decision variables identified as the main driving forces of energy and exergy in the previous sections are introduced to a genetic algorithm (GA) model to optimize the system performance in terms of energy and cost. GA is one of the main optimization approaches widely used to optimize multi-generation systems in recent years. Despite the simple concept behind the GA, it is a robust tool for optimizing sophisticated nonlinear or discrete systems performance. With coding in a specific interval, the GA considers each parameter as gen and the potential answers chromosomes. Various combinations of genes constitute a population of variable chromosomal structures. Table 5 contains the GA-related model parameters.

Table 5. GA structure parameters.

Parameter	Value
Population size	60
Individual number	18
Mutation probability	0.25
Maximum generation	72

The bi-objective GA model aims to simultaneously optimize the proposed system's exergy efficiency and total cost rate. The objective functions are defined as follows,

$$\eta_{ex,multi} = \frac{\dot{W}_{net} + \dot{W}_{wind} + \dot{m}_{32}(\dot{X}_{33} - \dot{X}_{32}) + \dot{m}_{27}(\dot{X}_{27} - \dot{X}_{28}) + \dot{X}_{H_2}}{\dot{X}_{in} + \dot{X}_{wind}} \quad \textbf{(32)}$$

$$\dot{X}_{in} = A_c I_c (1 + \frac{1}{3}(\frac{T_0}{T_s})^4 - \frac{4}{3}(\frac{T_0}{T_s})) \quad \textbf{(33)}$$

$$\sum \dot{Z}_k + \sum \dot{C}_f = \sum \dot{C}_p \quad \textbf{(34)}$$

$I_C$and$T_s$are the mean solar insolation and sun temperature which are considered to be 550 W/m^2 and 6000K, respectively. Using the implicit weighting, the objective function can be rewritten as follows,

$$MAXF = w_1(\eta_{ex,multi}) + w_2(1 - \sum \dot{C}_p) \quad \begin{cases} 0 \le w_1 \le 1 \\ 0 \le w_2 \le 1 \\ w_1 + w_2 = 1 \end{cases} \quad \textbf{(35)}$$

Where, $w_1$andw_2 are the corresponding weights of exergy and cost, respectively. Based on the exergy analysis, four parameters have been selected as decision variables: temperature of exiting flow from absorptive chiller $T_2$2, pinch point in the boiler, working fluid flow rate in the ORC $\dot{m}_{30}$, and the pressure of the inlet flow to the turbine $P_3$0 . Table 6 contains the acceptable intervals for the decision variables in the GA model

Table 6. acceptable intervals for the decision variables in the GA model.

Decision variable	Interval	Constraint type
Pinch point in the boiler (^oC)	10-30	Thermodynamically
T_{22} (^oC)	140-160	Thermodynamically
$\dot{m}_{30}$ kg/s	7-9	Techno-economic
P_{30} (kPa)	1000-3000	Thermodynamically

F. Fast Calculation of Thermal Loads in a Typical Building

The following equations are generally used for fast calculation of heating and cooling loads in a typical building:

$$Q_{heating} = A_{heating} \times 0.15 \quad \textbf{(36)}$$

$$Q_{cooling} = A_{cooling}/25 \quad \textbf{(37)}$$

Where A is the building area.

G. Model Verification

System modeling has been implemented in the EES environment. For this, the thermodynamic properties of Li- Br were adopted from the study of Patek and Komfar [2]. For the n-Octane case, the thermodynamic properties have been calculated based on the existing primary function in the EES software. Table 7 contains the input parameters for the computational model.

When it comes to the absorption refrigeration cycle, the results of this study bear a close resemblance to the study of Iranmanesh and Mehrabian [10]. Results insist on the reliability of the developed model, as shown in Table 8.

4. RESULTS AND DISCUSSION

A. General Outcomes

This section provides the results of the exergy analysis for each component in the proposed system. As per Figure 2, the PTCs, boiler, hot water heat exchanger, and electrolyzer are the primary sources of exergy destruction in the cogeneration system, respectively. This is mainly due to the significant temperature difference between the PTCs and ORC working fluids. As shown in Figure 3, the absorber and generators are responsible for most exergy destruction in the refrigeration absorption cycle. Along with the temperature difference, the irreversibility due to the heating and mixing of refrigerants and absorbents exacerbate the exergy destruction in the absorbent and generators. Table 9 provides the exergy and exergoeconomic results of the proposed system.

Table 7. Input parameters' values

Parameter	Value
Isentropic efficiency of the turbine	80
Isentropic efficiency of the pump	80
High-temperature heat exchanger efficiency	50
Low-temperature heat exchanger efficiency	50
Electrolyzer efficiency	65
Power capacity factor of wind turbine	60
Wind velocity ($\frac{m}{s}$)	5.5
Wind turbine diameter (m)	34
Solar insolation ($\frac{W}{m^2}$)	550
Inlet flow pressure to the turbine (kPa)	2000
Pinch point in the boiler (^oC)	20
Pinch point in the high-temperature generator(^oC)	5
Pinch point in the low-temperature generator(^oC)	10
Pinch point in the condenser (^oC)	5
Pinch point in absorber (^oC)	5
Pinch point in the evaporator (^oC)	3
Sun temperature T_s (K)	6000
Inlet water flowrate to electrolyzer (^oC)	6000
T_0 (^oC)	25
T_{34} (^oC)	327
T_{21} (^oC)	150
T_{23} (^oC)	25
T_{25} (^oC)	25
T_{27} (^oC)	12
Inlet water flowrate to electrolyzer ($\frac{KG}{S}$)	1
$\dot{m}_1(\frac{KG}{S})$	1
$\dot{m}_{23}(\frac{KG}{S})$	12
$\dot{m}_{25}(\frac{KG}{S})$	14
$\dot{m}_{27}(\frac{KG}{S})$	20
$\dot{P}_0$ (kPa)	101.3

Table 8. Verification of the double-effect LiBr-H_2O absorption refrigeration cycle with the study ofIranmanesh and Mehrabian [10]

	This study	Iranmanesh and Mehrabian [?]
$\dot{Q}_{evap}(KW)$	354.2	354.3
$\dot{Q}_{gen}(KW)$	265.4	265.5
$\dot{Q}_{abs}(KW)$	436.01	436.18
COP	1.32	1.32
$T_{max}(^{o}C)$	150	150
$P_{max}\ (kPa)$	64.29	64.28
$P_{min}\ (kPa)$	0.88	0.88

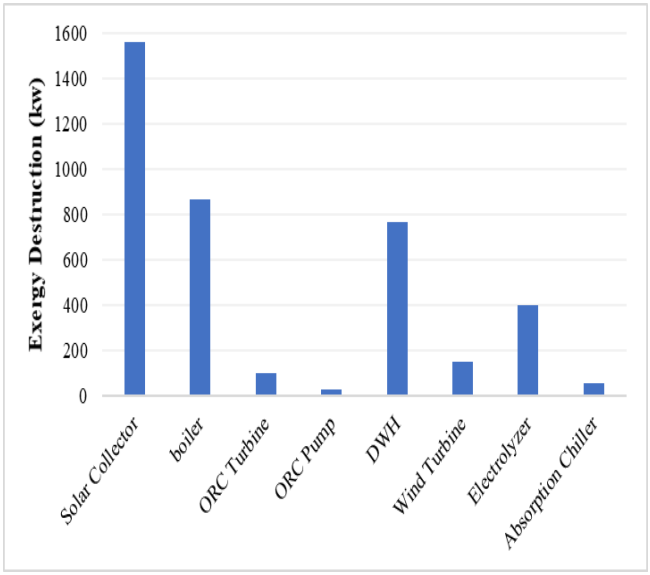

Fig. 2. Exergy destruction rate of the cogeneration system components

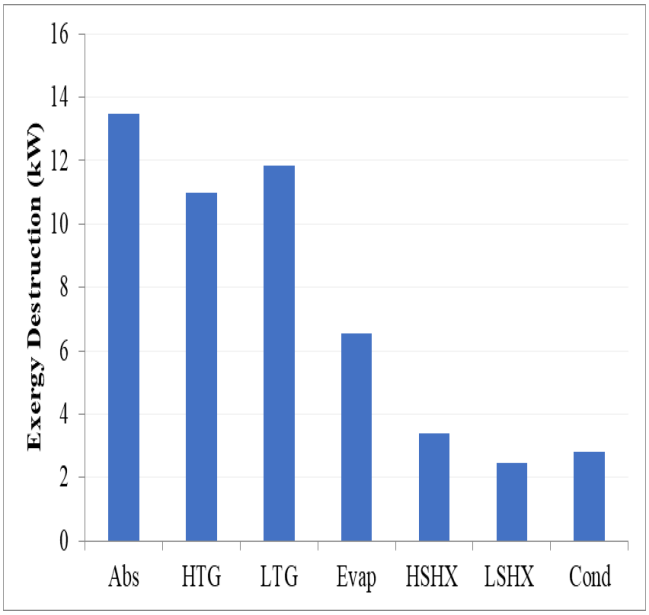

Fig. 3. Exergy destruction rate for the elements of the refrigeration absorption cycle

Table 9. The production capacity of the multi-generation system, efficiency, and exploitation rate of energy and exergy for the proposed system

Parameter	Value	Parameter	Value
$\dot{Q}_{evap}(KW)$	354.2	η_{multi}	%1.152
$\dot{Q}_{Heat}(KW)$	4073	$\eta_{ex,el}$	%10.17
$\dot{W}_{net}(KW)$	641.7	$\eta_{ex,cog,h}$	%29.73
$\dot{W}_{wind}(KW)$	222.1	$\eta_{ex,cog,c}$	%11.97
$\dot{m}_{H2}(\frac{KG}{S})$	0.0039	$\eta_{ex,trig}$	%41.15
$\dot{m}_{H2}(\frac{KG}{S})$	461.8	$\eta_{ex,multi}$	%51.83
$\dot{m}_{DWH}(\frac{KG}{S})$	23.3		
η_{el}	%13.88	$\dot{X}wind(KW)$	370.1
$\eta_{cog,h}$	%94.62	COP	%1.32
$\eta_{cog,c}$	%20.08	COP_{ex}	%24
η_{trig}	%99.23	$\dot{C}_{P,total}(\frac{\$}{S})$	0.02134
$A_{Heating}\ (m^2)$	23275	$A_{eCooling}\ (m^2)$	2500

According to the results, the system has better performance in terms of energy and exergy in cogenerating electricity and heating than power and cooling. The system is also of excellent performance in the tri-generation of electricity, heat, and cooling; however, the system's energy efficiency is much higher than the exergy efficiency in this case. Results also show that the energy exploitation rate of the system in the case of multi-generation is much higher than its exergy exploitation rate in other previous studies. It appears that the system is of a much higher potential for meeting the heating demand of a typical building rather than its cooling demand.

B. Parametric Studies on the Variable Parameters

B.1. Impact of Inlet Flow Pressure to the Turbine on the Exergy Efficiency and Production Cost Rate of The Tri-Generation System

Figure 4 illustrates the impact of inlet flow pressure on the turbine on the exergy efficiency of the system in the case of generating electricity, heating, and cooling. Findings suggest that with the increase of the inlet flow pressure to the turbine, the exergy efficiency and cost rate of the system increase to a certain degree but then fall into a declining trend. Working under pressures higher than 2200 kPa demand requires higher pump work that brings about exergy destruction in the tri-generation system.

B.2. Impact of Inlet Flow Pressure to the Turbine on The Rate of Exergy Exploitation and Production Cost Rate of the Multi-Generation System

Figure 5 shows the impact of inlet flow pressure to the turbine on the rate of exergy exploitation in the case of multi-generation. As shown in Figure 5, the rate of exergy exploitation increases by the pressure of 2600 kPa but falls into a declining trend afterward.

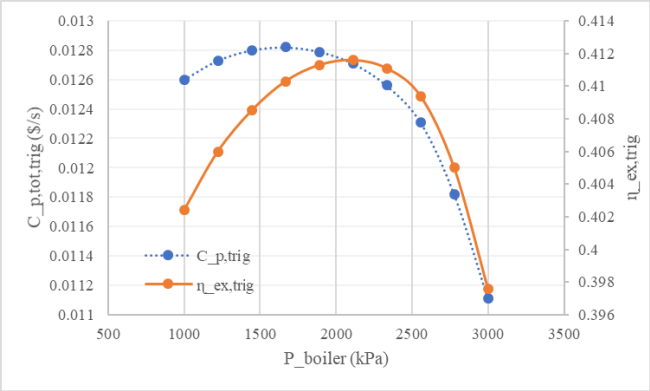

Fig. 4. The turbine's impact of inlet flow pressure on the tri-generation system's exergy efficiency and production cost rate.

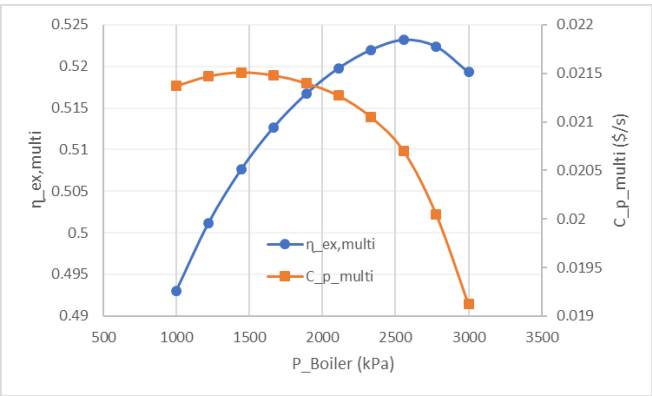

Fig. 5. . Impact of inlet flow pressure to the turbine on the rate of exergy exploitation and production cost rate of the multi-generation system.

B.3. Impact of Pinch Point in the Boiler on the Exergy Exploitation and Production Cost Rate of the Multi-Generation System

Figure 5 illustrates the influence of the pinch point in the boiler on the exergy exploitation and production cost rate of the multi-generation system. As shown in figure 5, the increase of the pinch point temperature in the boiler has adverse effects on both the exergy exploitation and production cost rate of the multi-generation system. This is mainly due to the reduction of entering heat to the boiler, which lowers the temperature of the inlet flow rate to the turbine and reduces the power generation capacity. As the working fluid exit the turbine at lower temperatures, the heat recovery rate in the deployed heat exchanger is also reduced. It brings about more exergy destruction in the proposed system. However, the lower pinch point temperature in the boiler provides an opportunity to reduce the size of the heat exchanger and decrease the initial investment costs.

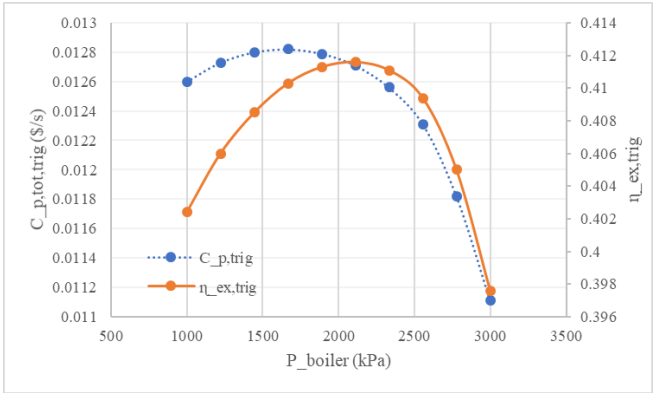

Fig. 6. Impact of pinch point in the boiler on the exergy exploitation and production cost rate of the multi-generation system

B.4. Impact of Exiting Flow Temperature From the Absorptive Chiller Generator on the Exergy Exploitation and Production Cost Rate of the Multi-Generation System

Figure 6 presents the impact of exiting flow temperature from the absorptive chiller generator on the multi-generation system's exergy exploitation and production cost rate. Based on the outcomes, the increase of the inlet flow temperature to the ORC has an increasing effect on the rate of exergy exploitation in the proposed system. With the rise of temperature from 140 to 156, the COP of the absorptive chiller increases, bringing about higher power generation capacity and exergy exploitation rate in the system. Contrary to the exergy exploitation rate, rising the inlet flow temperature to the ORC seemingly hurts the cost rate of the proposed system, which is mainly to the reduction of exergy destruction rate in the boiler.

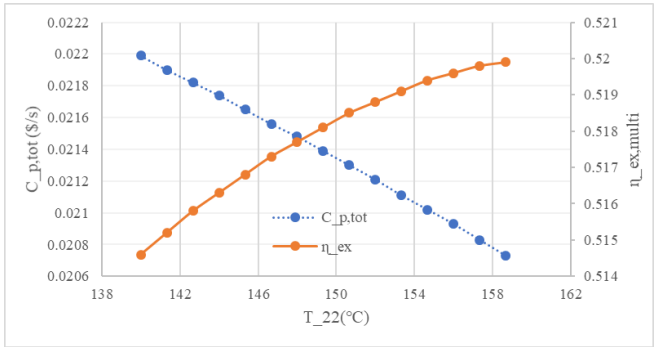

Fig. 7. Impact of exiting flow temperature from the absorptive chiller generator on the multi-generation system's exergy exploitation and production cost rate.

B.5. Impact of Working Fluid Flow Rate in the Orc on the Exergy Exploitation and Production Cost Rate of the Multi-Generation System

Figure 7 illustrates the impact of ORC Working fluid flow rate on the multi-generation system's exergy exploitation and production cost rate. An increase of the flow rate of working fluid in the ORC brings about higher electricity generation and hydrogen production capacity, and accordingly, more exergy exploitation rate in the proposed cycle; but, it requires enlarging the size of equipment such as heat exchangers that further exacerbate the production cost rate in the proposed system.

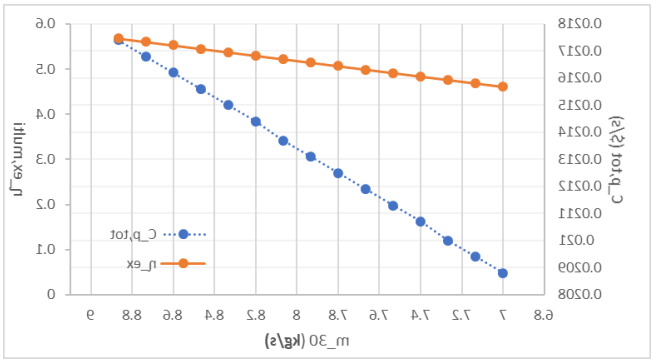

Fig. 8. Impact of working fluid flow rate in the ORC on the exergy exploitation and production cost rate of the multi-generation system.

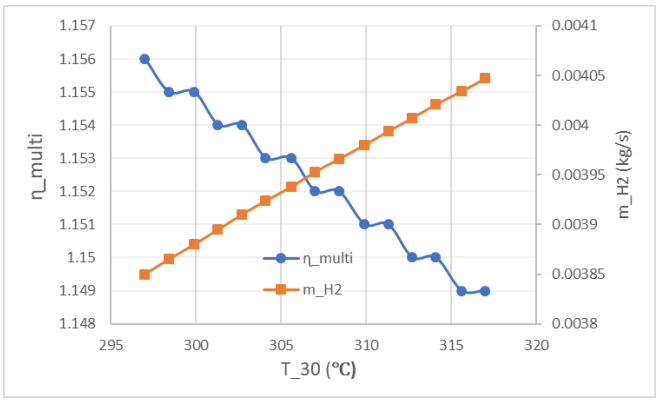

Fig. 10. Impact of entering flow temperature to the turbine on the hydrogen production rate and energy exploitation in the proposed system.

B.6. Impact of Entering Flow Temperature to the Turbine on the Exergy Exploitation and Production Cost Rate of the Multi-Generation System

Figure 8 demonstrates the effect of inlet flow temperature to the turbine on the multi-generation system's exergy exploitation and production cost rate. As the increase of inlet flow temperature to the turbine leads to higher work generation, and therefore, higher exergy exploitation rate in the cycle; however, the effect, on the other hand, harms the cost rate of the proposed system, as it needs larger equipment to provide such rate of exergy improvement.

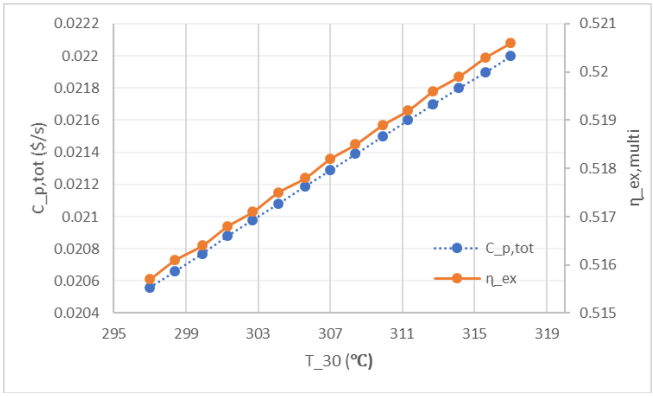

Fig. 9. . Impact of entering flow temperature to the turbine on the exergy exploitation and production cost rate of the multi-generation system.

B.7. Impact of Entering Flow Temperature to the Turbine on the Rate of Hydrogen Production and Energy Exploitation in the Proposed System

Figure 9 illustrates the influence of entering flow temperature to the turbine on the rate of hydrogen production and energy exploitation in the proposed system. As per the graph, raising the temperature of inlet flow to the ORC turbine hurts the energy exploitation rate of the system. However, it increases the rate of hydrogen production on the other hand.

B.8. Effects of Inlet Flow Temperature to the Absorptive Chiller on the Exergy Destruction Rate, COP, and Exergy Efficiency of the Chiller

Figure 10 evaluates the effects of inlet flow temperature on the absorptive chiller on the chiller's exergy destruction rate, COP, and exergy efficiency. Rising the inlet flow temperature brings about a higher temperature difference, and therefore, a higher exergy destruction rate in the chiller. As a result, the measure may lower the exergy efficiency of the chiller and reduce the exergitical performance of the proposed system. This is while the chiller's COP shows an insignificant sensitivity to changing the inlet flow temperature.

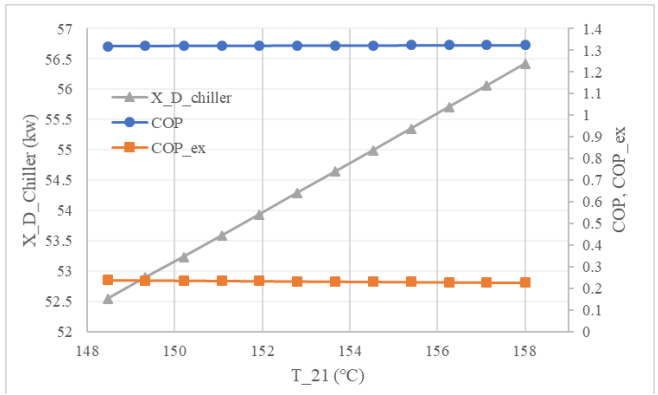

Fig. 11. Effects of inlet flow temperature to the absorptive chiller on the exergy destruction rate, COP, and exergy efficiency of the chiller.

B.9. Impact of Wind Velocity on the Exergy Destruction Rate of the Wind Turbine and Exergy Exploitation Rate of the Multi-Generation System

Figure 11 assesses the impact of wind velocity on the exergy destruction rate of the wind turbine and the exergy exploitation rate of the multi-generation system. Findings suggest that the exergy destruction rate of the wind turbine exponentially increases with the increase of wind velocity. However, because of higher electricity production capacity, the energy exploitation rate of the proposed system increases with the rise of wind velocity.

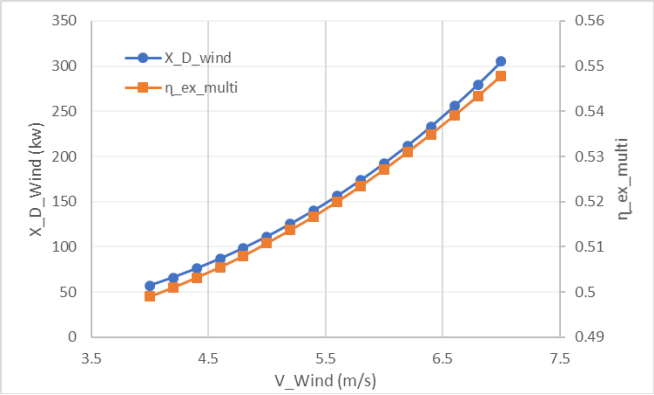

Fig. 12. Impact of wind velocity on the exergy destruction rate of the wind turbine and exergy exploitation rate of the multi-generation system.

5. OPTIMIZATION RESULTS

Sensitivity analysis shows that the selected decision variables have various impacts on the performance of the proposed system. Therefore, a bi-objective optimization model is needed to simultaneously optimize the performance of the proposed system both in terms of cost and exergy. A GA model has been adopted in this study to optimize the decision variables to maximize the exergitical performance of the system at the lowest cost. Table 10 provides the GA-related results for maximizing the rate of exergy exploitation and minimizing the production cost for the proposed system.

Table 10. GA optimization results.

	Base	Max $\eta_{ex,mu}$	Difference	Min $\dot{C}_{p,total}$	Difference	Multi-objective	
						Max(F)	Difference
$\eta_{ex,mu}$	0.5183	0.5442	5%	0.51	-1.3%	0.53	2.6%
$\dot{C}_{p,total}$	0.02133	0.02216	1%	0.0217	-17%	0.0203	-12.9%

As per Table 10, the two objective functions flatly contradict each other, as maximization of the exergy efficiency function maximizes the cost production rate, and minimization of the cost production rate slightly reduces the exergy efficiency rate of the proposed system. Therefore, a weighted objective function has been developed based on the two objective functions to find the most optimum decision variables for the simultaneous optimization of the system performance in terms of exergy efficiency and cost. Optimization results suggest a 2.6% improvement in the rate of exergy exploitation from the proposed system. Additionally, there is room for reducing the total rate of production cost by 12.9% with the optimization of the decision variables in the proposed system.

6. CONCLUSIONS AND SUGGESTIONS FOR THE FUTURE STUDIES

This paper has evaluated and optimized the performance of a renewable-assisted multi-generation system based on exergoeconomic. The proposed system is composed of PTCs, a horizontal-axis wind turbine, an organic Rankine cycle, heat recovery heat exchangers, a parallel double-effect LiBr-H_2O absorptive chiller, heat recovery heat exchangers, and an electrolyzer that has been designed for simultaneous production of electricity, heating, cooling, and hydrogen. So that, a thermodynamic model of the proposed system has been developed in the environment of the EES software; a GA model also has been developed to find the optimum composition of decision variables that efficiently optimize the system performance in terms of cost and exergy. In the case of energy analysis, the quality of the system performance can restrict the analysis results because the energy investigations cannot guarantee the system efficiency. However, exergy is the most useful indicator that can be gained from the amount of energy or the flow of materials in a quantified environment. To overcome the limitations of the first law of thermodynamics, the exergy analysis is an appropriate technique; because energy analysis provides no information about the amount of energy which vanishes in energy conversions and it doesn't count the usefulness or quality of the numerous energy and material streams. Searching for the primary exergy destruction sources, findings identify the boiler as the critical component that negatively affects this system's exergy efficiency. The significant temperature difference in the boiler brings about a high rate of irreversibility in this component and further exacerbates the exergy efficiency in the whole system. A sensitivity analysis also has been implemented to measure the impact of decision variables on the exergoeconomic performance of the proposed system. Based on the results, rising the inlet flow rate and inlet flow temperature to the ORC turbine increases the system's exergy efficiency and production cost rate. This is while the increase of the pinch point in the boiler and inlet flow temperature to the ORC pump brings about a negative impact on the production cost rate of the system. Results also suggest that the wind velocity harms the exergy destruction rate in the wind turbine, but positively impacts the rate of exergy exploitation from the proposed system. With the optimization of the decision variables using a GA model, it was found that there is room to enhance the exergy exploitation rate by 2.6% and reduce the total rate of the production cost of the proposed system by 12.9%.

REFERENCES

1. M. H. Jahangir, S. A. Mousavi, and M. A. V. Rad, "A techno-economic comparison of a photovoltaic/thermal organic Rankine cycle with several renewable hybrid systems for a residential area in Rayen, Iran," Energy Conversion and Management, vol. 195, pp. 244-261, 2019.
2. F. A. Boyaghchi and P. Heidarnejad, "Thermoeconomic assessment and multi objective optimization of a solar micro CCHP based on Organic Rankine Cycle for domestic application," Energy conversion and Management, vol. 97, pp. 224-234, 2015.
3. M. Asif and T. Muneer, "Energy supply, its demand and security issues for developed and emerging economies," Renewable and sustainable energy reviews, vol. 11, no. 7, pp. 1388-1413, 2007.
4. O. Siddiqui and I. Dincer, "Analysis and performance assessment of a new solar-based multigeneration system integrated with ammonia fuel

cell and solid oxide fuel cell-gas turbine combined cycle," Journal of Power Sources, vol. 370, pp. 138-154, 2017.
5. A. Modi, F. Bühler, J. G. Andreasen, and F. Haglind, "A review of solar energy based heat and power generation systems," Renewable and Sustainable Energy Reviews, vol. 67, pp. 1047-1064, 2017.
6. P. Ahmadi, I. Dincer, and M. A. Rosen, "Exergo-environmental analysis of an integrated organic Rankine cycle for trigeneration," Energy Conversion and Management, vol. 64, pp. 447-453, 2012.
7. R. Buck and S. Friedmann, "Solar-assisted small solar tower trigeneration systems," 2007.
8. F. A. Al-Sulaiman, I. Dincer, and F. Hamdullahpur, "Exergy modeling of a new solar driven trigeneration system," Solar Energy, vol. 85, no. 9, pp. 2228-2243, 2011.
9. R. Gomri, "Second law comparison of single effect and double effect vapour absorption refrigeration systems," Energy Conversion and Management, vol. 50, no. 5, pp. 1279-1287, 2009.
10. A. Iranmanesh and M. Mehrabian, "Thermodynamic modelling of a double-effect LiBr-H 2 O absorption refrigeration cycle," Heat and Mass Transfer, vol. 48, no. 12, pp. 2113-2123, 2012.
11. A. Salehzadeh, R. K. Saray, and D. JalaliVahid, "Investigating the effect of several thermodynamic parameters on exergy destruction in components of a tri-generation cycle," Energy, vol. 52, pp. 96-109, 2013.
12. D. Sonar, S. Soni, and D. Sharma, "Micro-trigeneration for energy sustainability: Technologies, tools and trends," Applied Thermal Engineering, vol. 71, no. 2, pp. 790-796, 2014.
13. S. Anvari, R. K. Saray, and K. Bahlouli, "Conventional and advanced exergetic and exergoeconomic analyses applied to a tri-generation cycle for heat, cold and power production," Energy, vol. 91, pp. 925-939, 2015.
14. A. Noorpoor and S. Heidararabi, "Exergoeconomic assessment, parametric study and optimization of a novel solar trigeneration system," International Journal of Renewable Energy Research (IJRER), vol. 6, no. 3, pp. 795-816, 2016.
15. A. Mousafarash, "Exergy and Exergoenvironmental Analysis of a CCHP System Based on a Parallel Flow Double-Effect Absorption Chiller," International Journal of Chemical Engineering, vol. 2016, 2016.
16. B. Eisavi, S. Khalilarya, A. Chitsaz, and M. A. Rosen, "Thermodynamic analysis of a novel combined cooling, heating and power system driven by solar energy," Applied Thermal Engineering, vol. 129, pp. 1219-1229, 2018.
17. P. Ahmadi, I. Dincer, and M. A. Rosen, "Development and assessment of an integrated biomass-based multi-generation energy system," Energy, vol. 56, pp. 155-166, 2013.
18. M. Al-Ali and I. Dincer, "Energetic and exergetic studies of a multigenerational solar–geothermal system," Applied Thermal Engineering, vol. 71, no. 1, pp. 16-23, 2014.
19. M. Malik, I. Dincer, and M. A. Rosen, "Development and analysis of a new renewable energy-based multi-generation system," Energy, vol. 79, pp. 90-99, 2015.
20. S. Ozlu and I. Dincer, "Development and analysis of a solar and wind energy based multigeneration system," Solar Energy, vol. 122, pp. 1279-1295, 2015.
21. İ. H. Yılmaz, K. Saka, and O. Kaynakli, "A thermodynamic evaluation on high pressure condenser of double effect absorption refrigeration system," Energy, vol. 113, pp. 1031-1041, 2016.
22. R. Maryami and A. Dehghan, "An exergy based comparative study between LiBr/water absorption refrigeration systems from half effect to triple effect," Applied Thermal Engineering, vol. 124, pp. 103-123, 2017.
23. M. Moghimi, M. Emadi, P. Ahmadi, and H. Moghadasi, "4E analysis and multi-objective optimization of a CCHP cycle based on gas turbine and ejector refrigeration," Applied Thermal Engineering, vol. 141, pp. 516-530, 2018.
24. G. Yang and X. Zhai, "Optimization and performance analysis of solar hybrid CCHP systems under different operation strategies," Applied Thermal Engineering, vol. 133, pp. 327-340, 2018.
25. N. Sezer and M. Koç, "Development and performance assessment of a new integrated solar, wind, and osmotic power system for multigeneration, based on thermodynamic principles," Energy Conversion and Management, vol. 188, pp. 94-111, 2019.
26. F. Yilmaz, M. Ozturk, and R. Selbas, "Energy and exergy performance assessment of a novel solar-based integrated system with hydrogen production," International Journal of Hydrogen Energy, vol. 44, no. 34, pp. 18732-18743, 2019.
27. R. Gomri and R. Hakimi, "Second law analysis of double effect vapour absorption cooler system," Energy conversion and management, vol. 49, no. 11, pp. 3343-3348, 2008.
28. L. G. Farshi, S. S. Mahmoudi, and M. Rosen, "Exergoeconomic comparison of double effect and combined ejector-double effect absorption refrigeration systems," Applied Energy, vol. 103, pp. 700-711, 2013.
29. J. Patek and J. Klomfar, "A computationally effective formulation of the thermodynamic properties of LiBr–H2O solutions from 273 to 500 K over full composition range," International journal of refrigeration, vol. 29, no. 4, pp. 566-578, 2006.